

Effect of the Catalytic Aquathermolysis Process on the Physicochemical Properties of a Colombian Crude Oil

Keyner S. Núñez-Méndez, Luis M. Salas-Chia, Daniel Molina V,* Samuel F. Muñoz, Paola A. León, and Adan Y. León



Cite This: <https://dx.doi.org/10.1021/acs.energyfuels.0c04142>

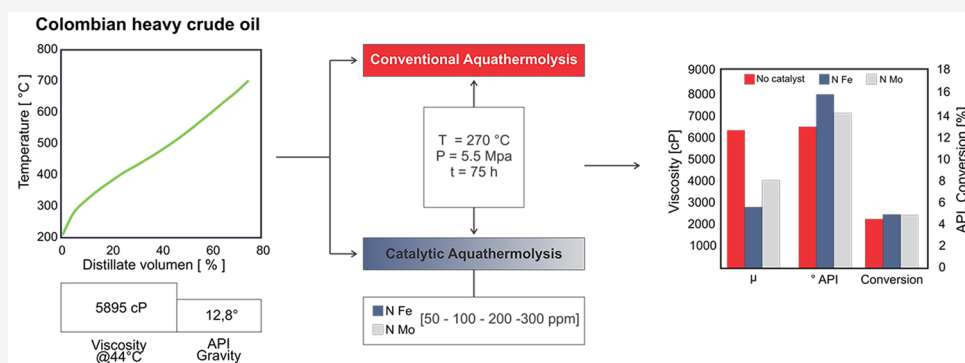


Read Online

ACCESS |

Metrics & More

Article Recommendations



ABSTRACT: In this work, the catalytic aquathermolysis process of a Colombian heavy crude oil was studied. Reactivity tests were conducted in a microbatch reactor at 270 °C and saturation pressure of 5.5 MPa, during 66 h, using iron and molybdenum naphthenates in concentrations of 50–300 ppm as catalysts. The use of these catalysts reduced the gas yield from 1% to 4.2% w/w, the viscosity from 10% to 52.3% with iron naphthenate, and from 11.6% to 31.4% with molybdenum naphthenate. Crudes subjected to catalytic aquathermolysis increased their API gravity from 1.1 to 2.5 and 0.5 to 1.8 units, showing a significant decrease in complex fractions with boiling points above 340 °C and conversions in the order of 7% and 8% with respect to the precursors of molybdenum and iron naphthenates. Unlike other studies, the changes in the physical properties were correlated with changes in the chemical structure by ATR-FTIR spectroscopy. The average molecular parameters showed that the greatest differences with respect to the base crude oil were the length of the alkyl chains, the aromaticity, and the sulfuration. Results indicate different characteristics from the catalysts being studied, with iron naphthenate yielding better favorable effects in the change of the physicochemical properties of the improved crude oils. The experimental methodology proposed in this work indicates that the catalytic aquathermolysis process is a recovery method that allows for improving the properties of the crude oils, under reservoir conditions, due to the formation of products of smaller size and molecular weight.

1. INTRODUCTION

Heavy and extra-heavy crude oil reserves represent around 70% of the recoverable crude oil worldwide and have become the focus of attention to supply the world energy demand,¹ but due to the low API gravity, high viscosity, and high content of heteroatoms such as sulfur, nitrogen, and oxygen in this type of oil,^{2–4} primary and secondary recovery methods have low efficiency in the production. For this reason, different enhanced oil recovery (EOR) methods have been implemented with numerous ongoing heavy and extra-heavy oil projects, reaching an associated production of approximately 2 million barrels per day.⁵ Thermal EOR methods (THEOR) play an important role in enhanced oil recovery,^{6–9} because of representing around 47.7% of the enhanced recovery methods,¹⁰ and are focused on reducing the viscosity of the

crude oil in the reservoir to increase its mobility and facilitate its production through the addition of a hot fluid.

THEOR methods include hot water injection (HWF), continuous steam injection (SD), cyclic steam injection (CSS), steam-assisted gravitational drainage (SAGD), and in situ combustion (ISC), among others, but steam injection methods are widely used since they have proven to be very successful worldwide for decades.^{10–12} However, these methods have

Received: December 8, 2020

Revised: February 17, 2021

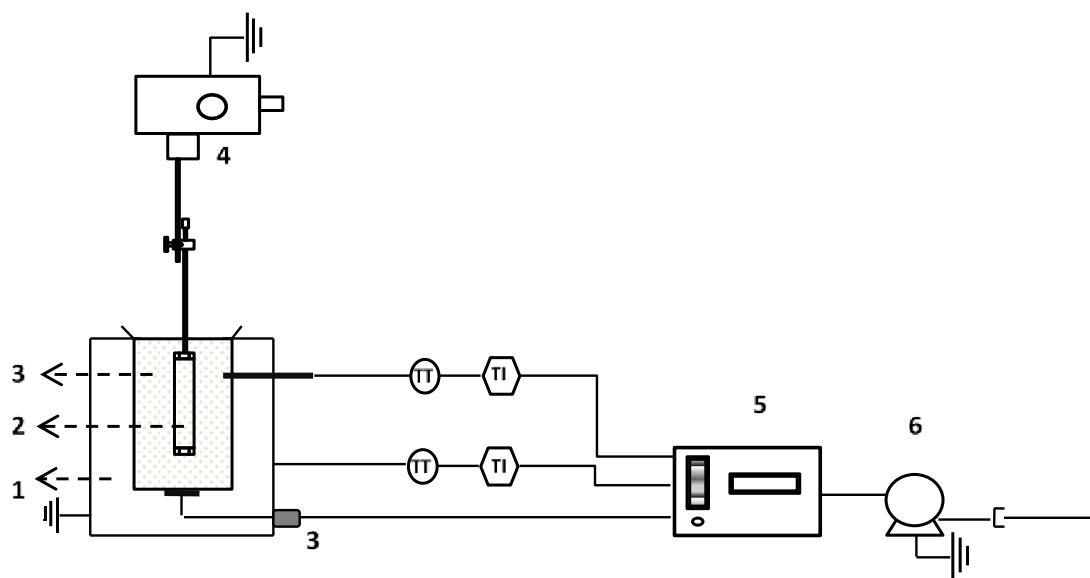


Figure 1. Schematic of the thermal bath and reactor used for the catalytic aquathermolysis tests: (1) fluidized sand bath, (2) batch reactor, (3) sand (Al_2O_3), (4) mechanical stirrer, (5) temperature control, and (6) compressor.

40 some operational problems that reduce the recovery factor
41 between 15% and 20%.¹ The first problem is the loss of
42 approximately 25% of the injected energy, depending on the
43 conditions of each reservoir,¹³ and second problem is the high
44 production of acid gases, such as H_2S and CO_2 , that causes
45 corrosion and possible unfavorable effects on the environ-
46 ment.^{14–16}

47 From this in situ gas generation, it has been possible to show
48 that the presence of steam on the petroleum produces
49 chemical changes, called aquathermolysis reactions, as
50 proposed by Hyne,¹⁷ who determined that there are
51 intermediate reactions such as hydrolysis, water–gas shift
52 (WGS), and hydrodesulfurization, which are generated due to
53 the oil–steam chemical interaction and the reservoir minerals.
54 Generally, aquathermolysis reactions occur in the temperature
55 range between 200 and 325 °C, in which hydrocarbons with a
56 wide distribution of molecular weights are produced. Although
57 preliminary studies showed that the production of gases
58 negatively affects the crude oil quality, subsequent studies
59 showed that the changes generated in the crude oil correspond
60 to an in situ upgrading.^{18–20} Thus, the conditions in the
61 process, the nature of the crude oil, the substrate, and the
62 steam quality, play important roles in the physicochemical
63 properties of the improved crude oil.

64 Considering the reactions and compounds generated during
65 the aquathermolysis, the addition of catalysts was proposed as
66 an optimized alternative to the conventional steam injection
67 method.^{21–23} The usage of catalysts with transition metal
68 precursors (iron, nickel, molybdenum, tungsten, cobalt, zinc),
69 in the presence of hydrogen and sulfur, decreases the activation
70 energy required for reactions in lower temperatures and
71 reaction times to take place. Different chemical compounds
72 have been developed and studied to act as a catalytic system in
73 the reactions of aquathermolysis. In general, catalysts have
74 been classified into heterogeneous and homogeneous.
75 Homogeneous catalysts are divided into soluble in water,
76 such as the salts of molybdenum, tungsten, iron, nickel, cobalt,
77 and soluble in oil, such as molybdenum naphthenate, iron
78 pentacarbonyl, and chromium *tert*-butyl alcohol, among
79 others.^{24–31}

To implement this process in the oil field, so as to
consolidate it as a hybrid technology, different fundamental
operational parameters must be analyzed, like some research
works that have evaluated different parameters and their
influence on the results: kind of reactor, temperature, residence
time, and type of catalyst.^{32–38} These works use a base crude
oil, with known characteristics, and carry out an experimental
design capable of evaluating the sensitivity of the variables
under study. As an example, for a heavy crude oil treated at
260 °C during 72 h, the viscosity reduced 46.2%, and the API
gravity increased 3 units.²² Several authors have determined
that the aquathermolysis on heavy crude oils, under a
temperature of 320 °C and reaction times around 72 h, allows
viscosity reductions of 33% with an increase in API gravity of
approximately 4 units. Regarding the recovery of liquids or
improved crude oils in the presence of catalysts in the
laboratory, an increase of around 15% was demonstrated with
respect to tests in the absence of a catalyst.^{37,39–42}

To evaluate the physicochemical changes of the upgraded
crude oil, different characterization techniques have been used,
among which the measurements of density, viscosity, simulated
distillation, thermogravimetry, elemental analysis, and SARA
compositional analysis (saturated, aromatic, resins, and
asphaltenes) stand out.^{31,34,40} To determine the average
chemical structure of crude oils and their products, analytical
techniques have been used, including nuclear magnetic
resonance (NMR), infrared (FTIR) and ultraviolet (UV–vis)
spectroscopy, X-ray diffraction (XRD), transmission electron
microscopy (TEM), scanning electron microscopy (SEM), X-
ray energy dispersive spectroscopy (EDX), and X-ray photo-
electron spectroscopy (XPS), among others.^{35,36,38,43–45} Due
to the variability of the physicochemical properties of the heavy
crude oils and their fractions, there is a significant difference in
their nature, and in consequence, their characterization
becomes complex.

The role of catalytic agents in aquathermolysis does not
occur directly. The mixtures that are used in the experimental
tests and are injected in the reservoir are precursors. At a
certain temperature and in the presence of organosulfuric
compounds, precursors are converted into metallic sulfides. 119

The formation of metallic sulfides and their presence in produced crude oil would make it possible to recycle these catalytic compounds and their use in upstream and downstream processes. On the other hand, pilot tests of the technology have been carried out, reporting favorable results for production increasing and upgrading oil. However, the massification to a commercial scale has not yet been done.^{46–50}

Catalytic aquathermolysis technology is fundamentally dependent on the catalyst used and the concentration supplied. Therefore, there is a need to evaluate the appropriate concentration of the catalyst to be applied in the recovery of typical Colombian heavy crude oils. Consequently, this research aims to study the effect of the variation in the metal ion concentration of iron naphthenate and molybdenum naphthenate on physicochemical properties of upgraded crude oils, such as density, viscosity, and percentage of light hydrocarbons conversion. Furthermore, the compositional variation of the crude oil is analyzed using average molecular parameters from ATR-FTIR and UV–vis spectroscopy techniques.

2. EXPERIMENTS

2.1. Materials. For the aquathermolysis tests, a Colombian heavy crude oil with an API gravity of 12.8 and a viscosity of 5895 cP (at 44 °C) was used. The catalysts used for this research were organic salts according to the efficiency recorded by this type of catalyst in previous studies. From a commercial point of view and taking into account the rock–fluid interaction, it is necessary to mix the catalyst in an additional solvent or organic compound.²⁷ Along with salts of iron naphthenate (6% iron, Strem Chemicals) and molybdenum naphthenate (6% of molybdenum). Molybdenum naphthenate was synthesized following the methodology reported by León et al.⁵¹ The catalyst was prepared by reaction between naphthenic acid (technical grade, Sigma-Aldrich, P/N 70340) and bis(acetylacetonate) dioxomolybdenum(VI) (Sigma-Aldrich, P/N 227749) mixed with a mass ratio of 3.74:1.

2.2. Catalytic Aquathermolysis Tests. A 170 cm³ batch reactor was used. The cylinder is 13.5 cm long and 4 cm in diameter, and it was constructed with Swagelok stainless steel accessories. The reactor works under isothermal and isochoric conditions at defined reaction times. The cylinder or reactor is connected to a variable speed motor that transmits a reciprocating rotational motion, immersed in a fluidized sand bath (Al₂O₃) that allows conducting the system heating. For the tests, a quantity of crude oil with a precursor (iron naphthenate or molybdenum naphthenate) is added at the estimated concentration and distilled water with a 2:1 mass ratio. Then, the reactor is pressurized with nitrogen at room temperature. Figure 1 shows a schematic of the reaction system used for aquathermolysis.⁵² The reactions were carried out at 270 °C, with a pressure of 5.51 MPa. The reaction time was 66 h. The aquathermolysis reactions without catalyst (no catalyst) were carried out under the same temperature, pressure, and reaction time conditions. The tests were carried out under the same temperature conditions, considering the operating window of the aquathermolysis reactions generated in the range from 200 to 300 °C.¹⁷ The pressure of 5.51 MPa at 270 °C guarantees the presence of saturated steam under reservoir conditions. The parameters according to the operating window of the conditions were established. Test conditions such as temperature, pressure, and reaction time were established, according to the process operating window and the applied parameters in other studies.^{53–55}

Catalytic aquathermolysis was investigated using oil-soluble catalysts (nickel and iron naphthenate). These catalysts have been applied in catalytic aquathermolysis studies with representative results in upgraded crude oil.^{56–58} The effect of the catalyst concentrations on 50, 100, 200 and, 300 ppm of metal ion was evaluated.

Subsequently, the reactor was cooled with an ice–water mixture and slowly depressurized. The treated crude oil was then separated

from the mixture by means of a Hettich Universal 320 R centrifuge with a speed of 15,000 rpm.

The mass balance was carried out by gravimetry, using the following equations

$$m_{\text{gas}(\text{final})} = m_{\text{R}(\text{initial})} - m_{\text{R}(\text{final})} \quad (1)$$

$$m_{\text{oil}(\text{final})} = m_{\text{oil}(\text{initial})} - m_{\text{gas}(\text{final})} \quad (2)$$

$$\% \text{gas} = \frac{m_{\text{gas}} \times 100}{m_{\text{gas}(\text{final})} + m_{\text{oil}(\text{final})}} \quad (3)$$

$$\% \text{oil} = \frac{m_{\text{oil}(\text{final})} \times 100}{m_{\text{oil}(\text{initial})}} \quad (4)$$

where $m_{\text{gas}(\text{final})}$ is the gas mass after reaction, $m_{\text{oil}(\text{initial})}$ is the crude oil mass before reaction, $m_{\text{oil}(\text{final})}$ is the crude oil mass after reaction, $m_{\text{R}(\text{initial})}$ is the reactor mass before reaction, $m_{\text{R}(\text{final})}$ is the reactor mass after reaction, %gas is the gas percentage after reaction, and %oil is the crude oil percentage after reaction, all in grams.

2.3. Characterization. **2.3.1. Viscosity.** Viscosity was measured with an Anton Paar rheometer, following the ASTM D7042 standard. A crude oil sample was placed between two parallel plates, and the shear stress of the crude was quantified along a temperature range between 20 and 50 °C. To determine the percentage of viscosity reduction with respect to the initial crude oil, the viscosity results were analyzed at 44 °C. The importance of quantifying the oil upgrading from its viscosity changes refers to the link of this property with the mobility relation and the flow of this phase in the porous medium.

2.3.2. ATR-FTIR Spectroscopy. The infrared spectrum was measured on a Bruker Tensor II FTIR spectrometer with an ATR cell and single-pass diamond reflection glass in the wavelength range between 400 and 4000 cm⁻¹.

2.3.3. UV–vis Spectroscopy. To obtain an adequate spectrum and considering the variability of the physicochemical properties of each crude oil, the appropriate sample concentration was determined in chloroform, in such a way that it was higher than a concentration that generates imperceptible peaks and lower than a concentration that presents too much noise. According to this premise and following the range established in the state-of-the-art method between 10 and 100 ppm,⁵⁹ the spectra were evaluated every 10 ppm, where the spectrum with a concentration of 60 ppm yielded the most adequate result. A quartz cell with a crude–solvent mixture was used in a Multiskan GO microplate spectrophotometer. The spectra were measured in the wavelength range between 200 and 600 nm. For each crude oil sample, the spectra were taken in triplicate.

2.3.4. Simulated Distillation. The simulated distillation curve was obtained following the ASTM D7169 standard. For this analysis, 0.2 g of crude oil was added to 10 mL of carbon disulfide (CS₂). Then, an aliquot of 1.5 mL of the previous solution was deposited in a vial, which was placed in a sample holder of an HP 6890 gas chromatograph.

3. RESULTS AND DISCUSSION

3.1. Heavy Crude Oil Characterization. Table 1 shows the characteristics of the Colombian base crude oil used to

Table 1. Properties of Colombian Heavy Crude Oil Used for Aquathermolysis

Property	Unit	Value
Density (°API)	g/cm ³	0.9806/12.8
Viscosity	cP at 44 °C	5895
$T_{5\%,\text{wt}}$	°C	278.7
$T_{20\%,\text{wt}}$	°C	381
$T_{30\%,\text{wt}}$	°C	430.3
$T_{50\%,\text{wt}}$	°C	535.5

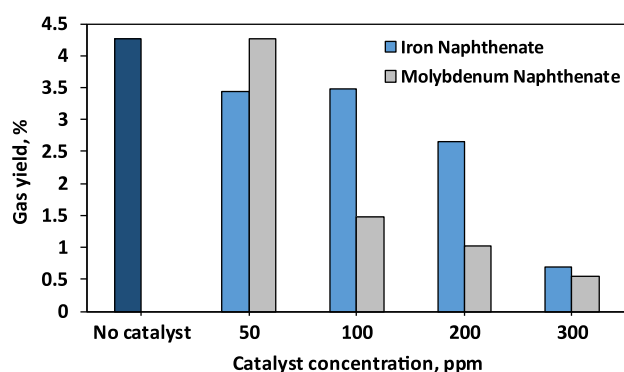


Figure 2. Percentage of gas yield from the catalytic aquathermolysis tests with different concentrations of iron and molybdenum naphthenate.

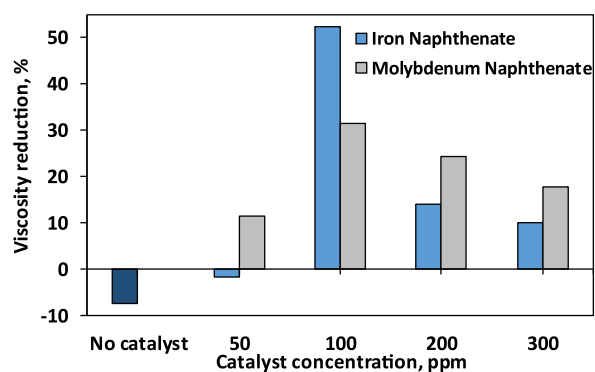


Figure 3. Percentage of viscosity reduction for different concentrations of iron and molybdenum naphthenate.

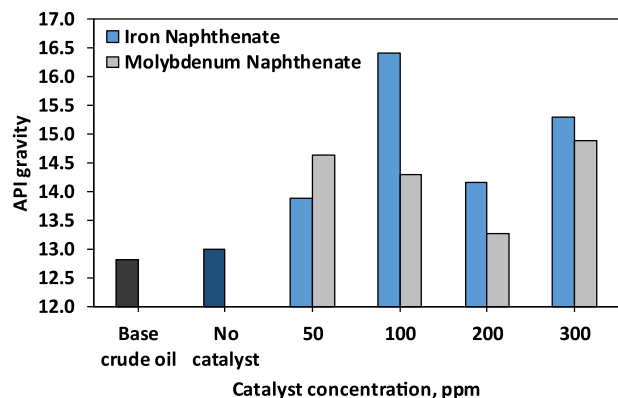


Figure 4. API gravity for upgraded crude oil improved via catalytic aquathermolysis under different concentrations of iron and molybdenum naphthenate.

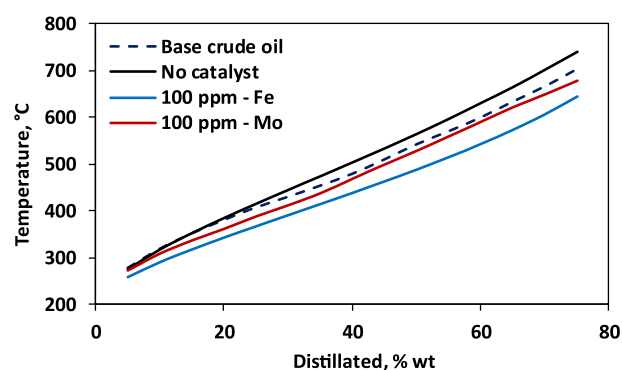


Figure 5. Distillation curves of the base crude oil and the upgraded crude oil under aquathermolysis conditions.

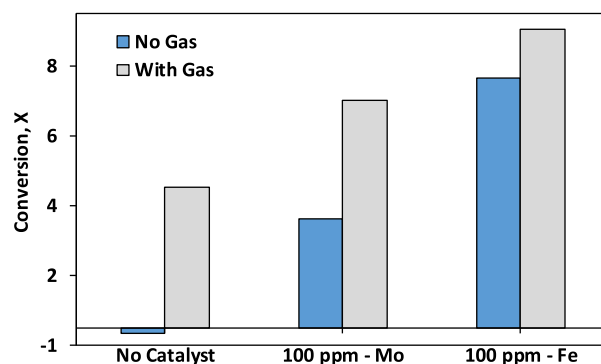


Figure 6. Conversion of the base crude oil and the upgraded crude oils obtained under aquathermolysis conditions.

The results (Figure 2) show that the gas yield decreases 244 proportionally with the increase in the concentration of the 245 catalysts. Metal sulfide catalysts split hydrogen H_2 molecules 246 into hydrogen free radicals, which react with crude oil to 247 obtain the upgraded crude oil. In general, the presence of 248 catalysts favors the combination of hydrogen free radicals and 249 hydrocarbon free radicals to form a stable molecule. In the 250 process, the condensation of hydrocarbon free radicals is 251 suppressed, and at the same time, the gas yield is reduced.⁶⁰ 252

From the results, it can be indicated that the catalytic 253 aquathermolysis conditions applied in this research imply an 254 improvement in the decrease in gas yield with respect to the 255 steam injection process. The sequence of the gas product yield 256 presented the following order: no catalyst < molybdenum 257 naphthenate < iron naphthenate. Thus, the trends of the 258 results can be attributed to the fact that each catalyst has a 259 selectivity according to the nature and reactivity of the crude 260 oil. With the molybdenum naphthenate tests, a greater 261 decrease in gas yield was obtained compared to iron 262 naphthenate when concentrations higher than 50 ppm were 263 used. These results follow the same trend reported in other 264 works, although both have a favorable effect on the properties 265 of the upgraded crude oil.^{21,61–63} 266

3.3. Quality Analysis of Crude Oils Obtained in the 267 **Catalytic Aquathermolysis Process.** Viscosity reduction is 268 one of the most representative evaluation parameters in an 269 upgraded crude oil since this property is closely related to the 270 physicochemical properties of the crude oil and to the mobility 271 ratio, directly representing a higher recovery factor.^{39,40,64} 272

Figure 3 shows the percentage of viscosity reduction of the 273 upgraded crude oils with respect to the base crude oil (at 44 274

233 study the effect of the concentration and nature of the catalyst 234 under steam injection conditions. These characteristics allow 235 us to establish that the selected crude corresponds to a heavy 236 crude oil.

237 **3.2. Colombian Crude Oil Reactivity under Catalytic** 238 **Aquathermolysis Conditions.** The percentage of gas yield is 239 estimated by the difference in the mass balance between the 240 initial crude oil and the liquid products obtained in the 241 reactivity tests. Figure 2 compares the results of the yield, in 242 percentage by weight of the gas, with respect to the base crude 243 oil, without and with catalyst, at different concentrations.

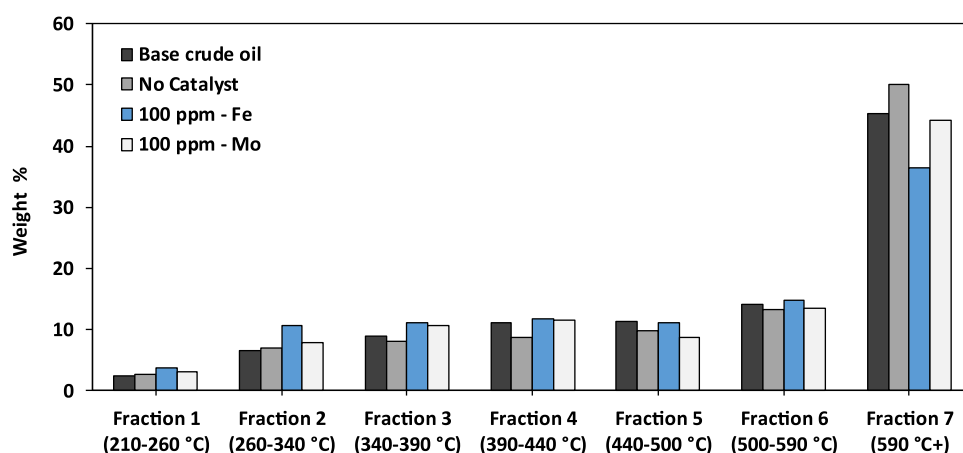


Figure 7. Representative fractions of the distillation curves of the base crude oil and the upgraded crude oils under aquathermolysis conditions.

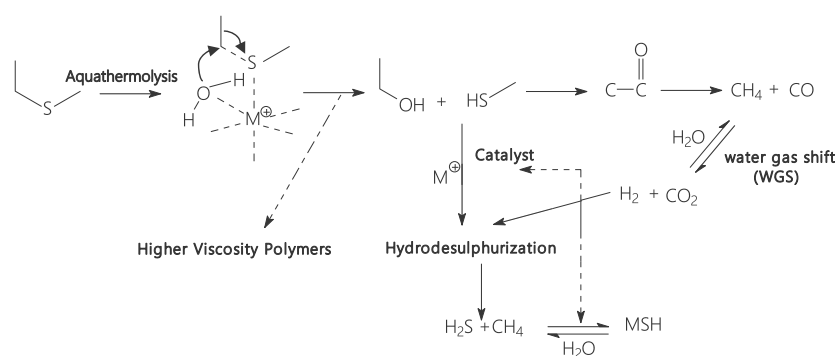


Figure 8. Reaction mechanism in catalytic aquathermolysis.

Table 2. Functional Groups Assignment in Infrared Spectroscopy

Intensity	Wavelength (cm ⁻¹)	Characteristic structure
1	747	Deformation of aromatic CH bonds out-of-plane =C-H (4H)
2	812	Deformation of aromatic CH bonds out-of-plane =C-H (2H or 3H)
3	870	Deformation of aromatic CH bonds out-of-plane =C-H (1H)
4	1033	Sulfoxides groups
5	1375	CH ₃ methyl group
6	1455	CH ₂ methylene group
7	1607	Aromatic C=C stretch
8	1707	Carboxylic group C=O stretch
9	2921	CH ₂ asymmetric stretch
10	2960	CH ₃ asymmetric stretch

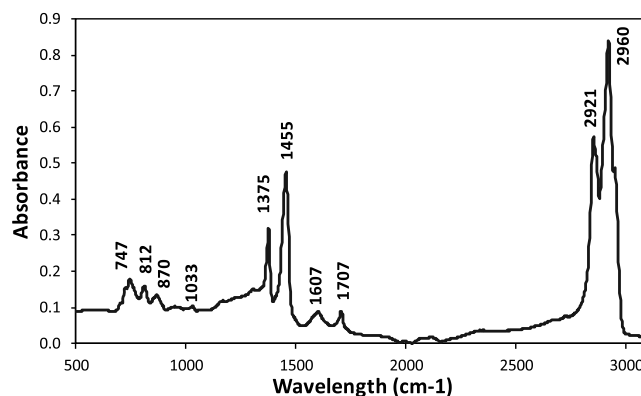


Figure 9. ATR-FTIR spectrum of the base crude oil.

275 °C). The test in the absence of catalyst showed an increase in
276 viscosity of 7.46%, possibly due to polymerization. This effect
277 occurs because of the instability and combination of the
278 hydrocarbon free radicals formed, which tend to create more
279 complex and branched molecules due to condensation
280 reactions.^{18,65}

281 The highest percentage of viscosity reduction was achieved
282 at 100 ppm of either iron or molybdenum naphthenate, with a
283 reduction of 52.3% and 31.4%, respectively. For the 200 and
284 300 ppm tests on the iron naphthenate precursor, a lower
285 reduction in viscosity is observed than that obtained at 100
286 ppm. According to the crude oil–water ratio, it is important to
287 consider that the sulfur content remains constant. Therefore,

the amount of catalyst formed depends on the sulfur content
288 available for the reaction (Figure 8). Another reason is that at
289 higher concentrations of the naphthenate salt, the organic
290 phase tends to participate in hydrogenation reactions, justified
291 by the additional hydrogen consumption. Further, the decrease
292 in the hydrogen content favors the combination of species,
293 which in the same way tends to form compounds of higher
294 molecular weight.^{32,61,63} This effect on the molybdenum
295 catalyst precursor is less pronounced because each catalyst
296 develops reactions of a different nature and intensity. The
297 results show that catalyst concentration plays an important role
298 in upgraded crude. The results presented trend with the works
299 reported by several authors. For example, the reduction of the
300 viscosity of heavy crude with a Citric-Fe(III) complex does not
301 change significantly above 2000 ppm.⁶⁶ 302

Table 3. Hydrocarbon Chemical Characterization Parameters from Infrared Spectroscopy^a

Parameter	Relationship
Aromaticity	$C1 = \frac{I_{1600}}{I_{747}}$
Oxidation	$C2 = \frac{I_{1710}}{I_{1455}}$
Branching	$C3 = \frac{I_{1375}}{I_{1455}}$
Paraffinicity	$C4 = \frac{(I_{747} + I_{1735})}{I_{1600}}$
Sulfurization	$C5 = \frac{I_{1030}}{I_{1465}}$
Degree of condensation	$C6 = \frac{I_{870}}{(I_{747} + I_{812})}$
Alkyl chain length	$C7 = \frac{I_{2927}}{I_{2957}}$

^aRepresented is the intensity of the absorbance band shown by the ATR-FT-IR spectrum at a wavelength specified *n*.

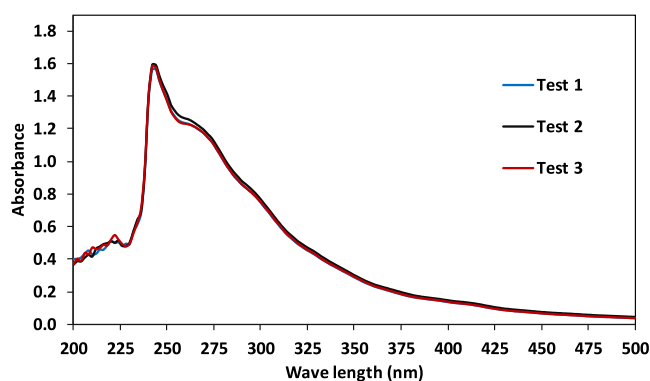


Figure 11. Calibration of UV-vis spectra for a representative base crude oil.

Figure 4 shows the API gravity of the upgraded crude oil obtained in this work. The results show that the aquathermolysis in the absence of catalyst shows a slight increase in API gravity, around 0.5 units with respect to the base crude oil, and this occurs due to the reactions of polycondensation and polymerization. The addition of metallic

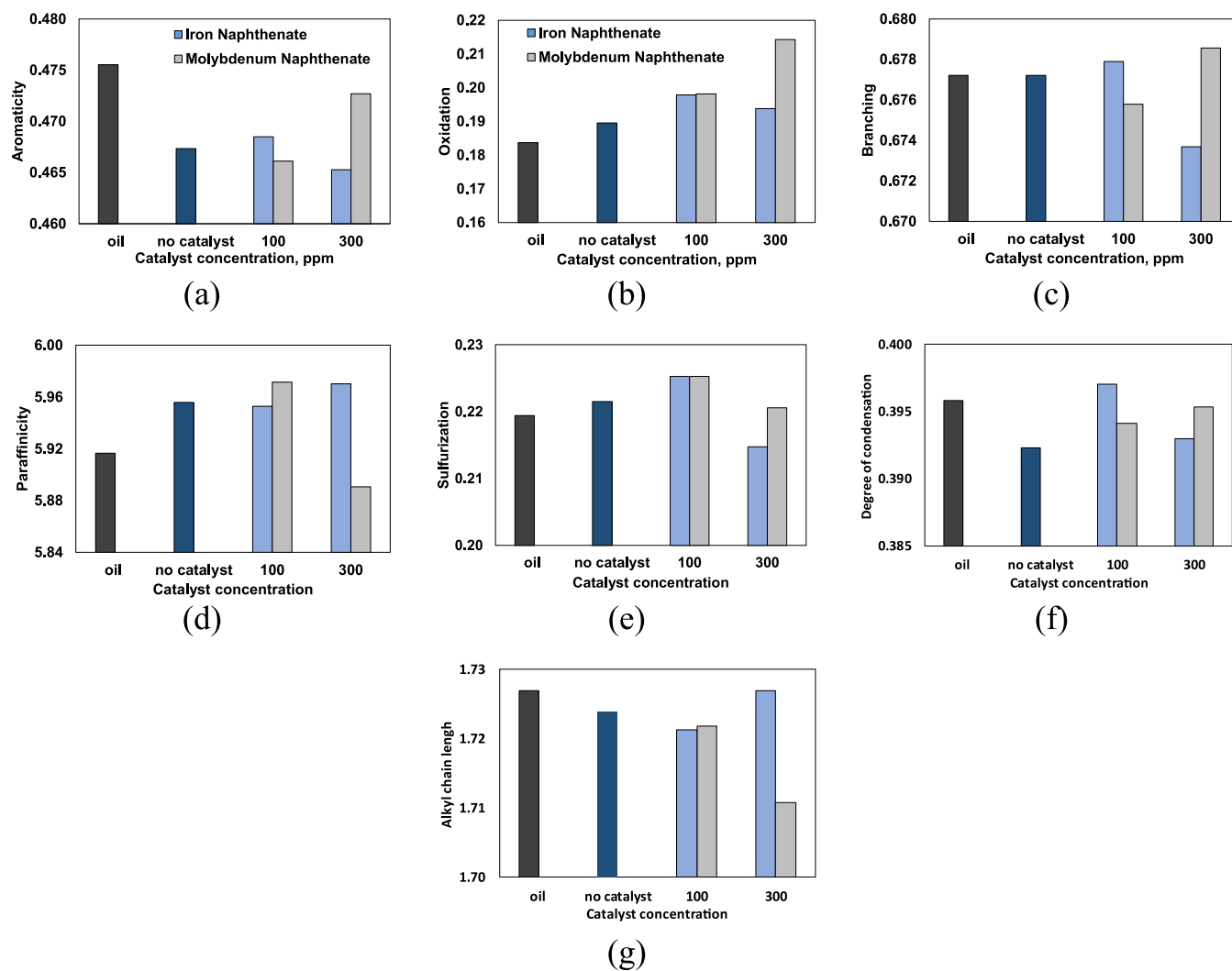


Figure 10. Characterization parameters, obtained by FTIR spectroscopy, of the upgraded crude oils under aquathermolysis conditions in the presence of iron naphthenate and molybdenum naphthenate: (a) aromaticity, (b) oxidation, (c) branching, (d) paraffinicity, (e) sulfurization, (f) degree of condensation, and (g) alkyl chain length.

Table 4. Absorbance, at Different Wavelengths, of the Upgraded Crude Oil via Aquathermolysis with Iron and Molybdenum Naphthenates

Catalyst concentration (ppm)	Benzene compounds (242 nm)		Naphthenic compounds (262 nm)		Porphyrin compounds (412 nm)	
	Fe	Mo	Fe	Mo	Fe	Mo
Base crude oil	1.589	1.589	1.252	1.252	0.129	0.129
Without catalyst	1.699	1.699	1.373	1.373	0.151	0.151
50	1.771	1.702	1.465	1.429	0.154	0.147
100	1.844	1.780	1.542	1.479	0.156	0.151
200	1.643	1.676	1.358	1.407	0.141	0.139
300	1.822	1.726	1.475	1.400	0.151	0.145

309 salt (precursor) in the reservoir yields metallic sulfides from
 310 the rupture of the R–S–R bond in aromatic and/or aliphatic
 311 structures. Furthermore, under favorable conditions, it is
 312 possible to obtain fewer complex structures, which favor the
 313 crude oil quality and its improved recovery. Nonetheless, the
 314 absence of hydrogen and catalyst leads to polycondensation
 315 and polymerization, which in turn, reduce the physicochemical
 316 quality of the crude.^{17,24,65,67}

317 Note that the 100 ppm iron naphthenate test attained the
 318 largest increase in API gravity, around 3.59 units. Meanwhile,
 319 for concentrations of 50, 200, and 300 ppm, the increase in
 320 API gravity was 1.6, 1.23, and 2.48 units, respectively. For
 321 molybdenum naphthenate, the greatest increase in API gravity,
 322 2.07 units, was observed at a concentration of 300 ppm.
 323 However, this increase is smaller than that with iron
 324 naphthenate for the same concentration. Likewise, for
 325 concentrations of 50, 100, and 200 ppm, the API gravity
 326 increased by 1.8, 1.47, and 0.45 units, respectively. In general,
 327 the results show that the API gravity of the upgraded crudes
 328 are higher with respect to the base crude and upgraded crude
 329 without catalyst. The changes can be attributed to the
 330 modifications of the chemical structure of the upgraded
 331 crude oil in each test due to the breaking of alkyl chains and
 332 multiple reactions. These results allow us to conclude that the
 333 two catalysts formed in situ have different selectivities, but
 334 both have a favorable effect on the properties of the upgraded
 335 crude oil.

336 According to the results obtained in viscosity and API
 337 gravity measures (Figures 3 and 4), the samples with the most
 338 representative changes in viscosity and density were selected to
 339 be analyzed by simulated distillation and ATR-FT-IR spec-
 340 troscopy characterization. In this investigation, the simulated
 341 distillation curves of the base crude and the upgraded crude
 342 oils under catalytic aquathermolysis conditions were studied.
 343 The purpose of this section was to determine the fractions
 344 yield behavior and its conversion with a boiling point above
 345 340 °C (340 °C+). Figure 5 compares the distillation curve of
 346 base crude oil and upgraded crude oils under aquathermolysis
 347 conditions with 100 ppm of metal ion, according to the highest
 348 efficiency in the tests. The trends of the crude oil distillation
 349 curves in the presence of a catalyst show significant differences
 350 with respect to the base crude oil and the crude obtained
 351 without catalyst.

352 The upgraded crude oils showed an increase in liquid
 353 products around 300 °C, being higher in the presence of iron
 354 naphthenate. From the distillation results it can be deduced
 355 that the presence of iron naphthenate produces a greater
 356 quantity of lower weight compounds compared to molybde-
 357 num naphthenate. On the other hand, the results show that
 358 under aquathermolysis conditions, but in the absence of a

359 catalyst, polycondensation reactions are favored, and therefore,
 360 compounds with higher boiling points are generated.

361 In this work, the fractions with the highest molecular weight
 362 in the crude oils and with boiling temperatures above 340 °C
 363 were considered. Therefore, it is important to evaluate its
 364 conversion, based on the liquid product yield produced with
 365 respect to the boiling point below 340 °C (340 °C–) during
 366 each of the aquathermolysis tests. To calculate the conversion
 367 at 340 °C (340 °C–), the following equation was used

$$X_{340^{\circ}\text{C}+} = \frac{(W_{340^{\circ}\text{C}+, \text{crude}} - W_{340^{\circ}\text{C}+, \text{liquids}}) \times 100}{W_{340^{\circ}\text{C}+, \text{crude}}} \quad (5)$$

368 where $X_{340^{\circ}\text{C}+}$ is the conversion of the base crude heavy
 369 fractions with temperatures above 340 °C (340 °C+), and
 370 $W_{340^{\circ}\text{C}+, \text{crude}}$ and $W_{340^{\circ}\text{C}+, \text{liquids}}$ are the fractions in the crude oil
 371 and liquid products, respectively. Figure 6 shows the
 372 conversion of the base crude oil and the respective upgraded
 373 crude oils.

374 To calculate the conversion of the 340 °C+ fraction, two
 375 scenarios are considered: first, the transformation toward
 376 liquids (without gas), and second, the conversion toward
 377 liquids and gases (with gas). The results show an increase in
 378 the conversion to liquid products when the tests are conducted
 379 in the presence of catalysts. However, when the conversion to
 380 liquids and gases is considered, the results show a greater
 381 increase with molybdenum than with iron naphthenate. On the
 382 other hand, the conversion obtained under aquathermolysis
 383 conditions, without the presence of acatalyst, yields a negative
 384 value. This can be attributed to the conditions that govern the
 385 free radical reactions, to the presence of the catalysts formed
 386 in situ, and to the hydrogen produced by the water–gas shift
 387 reactions.

388 Figure 7 shows the representative fractions of the distillation
 389 curves for this study, which were obtained following the ASTM
 390 D-7169 standard. Under aquathermolysis conditions, without a
 391 catalyst, an increase of the 590 °C+ fraction is observed.
 392 Meanwhile, for the upgraded crude oils in the presence of a
 393 catalyst, a significant increase is observed between fractions 1
 394 to 4. Comparing the upgraded crude oil with molybdenum
 395 naphthenate and the base crude oil, the light fractions of the
 396 former increase in the following order: fraction 4 > fraction 3 >
 397 fraction 2 > fraction 1. Also, when the crude oil is enhanced
 398 with iron naphthenate, the light fractions increase in the
 399 following order: fraction 2 > fraction 3 > fraction 4 > fraction
 400 1. On the other hand, for the two upgraded crude oils in the
 401 presence of a catalyst, the content of the complex fractions 590
 402 °C+ (vacuum bottoms) decreases in the reverse order.

403 The most complex compounds in crude oils, resins, and
 404 asphaltene are mainly concentrated in the 590 °C+ fraction.
 405 Thus, from the results, the transformation of fraction 7 can be

407 attributed to the reactivity of resins and asphaltenes under
408 catalytic aquathermolysis conditions, as indicated by other
409 authors.^{51,61,68} Figure 8 illustrates the general scheme of the
410 reaction mechanism proposed in the catalytic aquathermolysis
411 process, where it can be observed how the mechanisms are
412 interconnected. Thus, the product of one reaction can become
413 the raw material of another. The process also illustrates the
414 formation of organosulfur compounds, which can polymerize
415 or react with water to produce species that tend to participate
416 in a series of reactions.^{17,69} However, the presence of
417 precursors and water leads to polymerization inhibition with
418 the lower molecular weight formation.

419 **3.4. Characterization by ATR-FTIR and UV-Vis Spec-**
420 **trosopy.** An infrared spectrum represents the amount of
421 energy absorbed by the functional groups present in the
422 sample molecules. Given the large number of functional groups
423 present in hydrocarbons, several studies have identified specific
424 wavelengths where the absorbance intensity allows represent-
425 ing the functional groups and characteristic structures of crude
426 oils.^{42,70,71} Table 2 shows the wave numbers assignment
427 established in this research. Figure 9 was included in order to
428 define the wavelengths for the samples. To determine the
429 structural difference between the base crude oil and the
430 upgraded crude, characterization parameters were used.

431 From the functional groups identified, the parameters of
432 aromaticity, oxidation, branching, paraffinicity, sulfidation,
433 degree of condensation, and length of alkyl chains reported
434 by several authors were calculated.^{44,72} These parameters are
435 described in Table 3 and compared in Figure 10. The
436 parameters show that the aromaticity in the upgraded crude
437 oils decreases compared to the base crude oil. This can be
438 attributed to the reduction of C=C bonds. On the other hand,
439 the results show that concentrations of molybdenum
440 naphthenate higher than 100 ppm yield a decrease in gases,
441 which in turn reduces the breakdown of liquid products
442 (Figure 2). Meanwhile, the likelihood of aromatic hydrocarbon
443 free radical condensation increases.

444 An increase in the concentration of molybdenum naph-
445 thenate favors the formation of aromatic structures with a
446 higher content of branched linear structures. Upgraded crude
447 oils in the presence of the two catalysts, at 100 ppm, showed
448 insignificant differences with respect to the initial crude.
449 Meanwhile, higher concentrations of iron naphthenate favored
450 the formation of substituted aromatic compounds with alkyl
451 chains of greater length compared to molybdenum naph-
452 thenate.

453 The results show that the improved crude oil paraffinicity
454 grew in the presence of 100 ppm of catalyst. However, in
455 reactions with 300 ppm of molybdenum naphthenate, this
456 parameter significantly decreases. The paraffinicity grows
457 proportionally to the length of the alkyl chains located in the
458 aromatic species. Regarding the oxidation parameter, it
459 increases in all the samples relative to the base crude oil,
460 especially at 300 ppm of molybdenum naphthenate. It is well
461 known that catalysts act especially in the weakest bonds with
462 heteroatoms (C-R, R: S, O), causing reactions such as
463 oxygenation, alcoholization, and esterification.^{68,73,74} There-
464 fore, greater oxidation is associated with new species formation
465 with functional groups that contain oxygen and sulfur as
466 alcohols, ethers, esters, thioesters, thiols, and sulfoxides, among
467 others. This allows corroborating that oxidation reactions are
468 developed in the catalytic aquathermolysis tests carried out.

The maximum value of the sulfidation parameter in the 469
upgraded crude oils was obtained at 100 ppm of the metal ion 470
in the precursor, and at higher concentrations, it decreased. 471
This indicates that low concentrations of iron and 472
molybdenum naphthenate yield a lower concentration of 473
metal sulfide in the reaction. These results are attributed to the 474
oxidation of sulfides into sulfoxides. On the other hand, with 475
the increase in the concentration of the precursors of iron 476
naphthenate and molybdenum naphthenate, the oxidation of 477
sulfides decreases and the conversion of sulfur toward the 478
formation of metal sulfide improves. 479

The aromatic condensation parameter is related to 480
polyaromatic structures. As shown in Figure 10, this parameter 481
increases in the presence of precursors at 100 ppm, being 482
moderately higher for iron naphthenate. This indicates that at 483
low concentrations of metallic sulfide, the reactions are 484
governed by reactions between the radicals of the aromatic 485
rings. With the increase in the concentration of iron and 486
molybdenum naphthenate, species with a lower degree of 487
aromatic condensation are generated, possibly due to 488
desulfurization and hydrogenation reactions. 489

From the results obtained in this work, it is evident that the 490
most relevant parameters for the catalytic aquathermolysis are 491
the length of alkyl chains, the aromaticity, and the sulfurization 492
because these showed great differences between the initial and 493
the upgraded crude oil. Therefore, they agree with the 494
structural effect generated by the aquathermolysis in the 495
presence of catalysts. Thus, the variability of the results 496
depends on the nature and concentration of the catalyst 497
precursor, which produces a molecular change in the upgraded 498
crude oil. From the UV-vis spectra (Figure 11), the 499
wavelengths at 242, 262, and 412 nm, which represent the 500
concentration of benzene, naphthenic and porphyrin species, 501
respectively,⁵⁹ presented a standard deviation of 0.8%, 1.1%, 502
and 0.4%, respectively. 503

Table 4 shows the absorbances for the upgraded crude oils 504
obtained under aquathermolysis conditions in the presence of 505
iron and molybdenum naphthenate. The results show an 506
increase in the concentration of benzene and naphthenic 507
compounds in the tests within 50 and 100 ppm. However, in 508
this concentration range, the content of aromatic and 509
naphthene compounds is higher with iron than with 510
molybdenum, which allows the formation of lower molecular 511
weight species from structures with a higher degree of 512
complexity. 513

On the basis of the results of viscosity, API gravity, simulated 514
distillation, and the analysis of UV-vis and ATR-FTIR 515
spectroscopy, for the upgraded crude oils, it can be appreciated 516
that the difference in properties is related to the performance 517
and chemical composition of the products. In general, the 518
catalytic aquathermolysis is a recovery process that improves 519
the properties of crude oils in the reservoir and promotes the 520
formation of higher liquid yields due to the multiple reactions 521
to the presence of sulfur and to the participation of hydrogen 522
that yield compounds with a wide variety of size and molecular 523
weights. 524

4. CONCLUSIONS

During the aquathermolysis of heavy crude oils, molybdenum 525
naphthenate and iron naphthenate have different selectivities 526
and favor the conversion of complex compounds into 527
compounds of smaller molecular size, especially aromatic and 528
naphthenic compounds. 529

530 The steam injection process in the presence of iron
531 naphthenate, with a concentration of 100 ppm, showed an
532 outstanding 53% reduction in viscosity, greater light
533 components yield, and favorable physicochemical conditions.
534 Catalyst concentration plays an important role in upgraded
535 crude oil under catalytic aquathermolysis conditions. However,
536 an increase in the catalyst concentration does not always
537 generate a greater reduction in viscosity or improvement in the
538 physicochemical properties of the hydrocarbon. Although the
539 reactivity process due to the thermal effect is governed by free
540 radical reactions, the presence of hydrogen produced in the
541 process participates in the occurrence of multiple reactions that
542 improve the quality of the crude oil. Finally, the results of this
543 work indicate that the catalysts used have great potential in
544 recovery methods.

545 ■ AUTHOR INFORMATION

546 Corresponding Author

547 **Daniel Molina V** – Laboratorio de Resonancia Magnética
548 Nuclear, Universidad Industrial de Santander-UIS, A.A. 678
549 Bucaramanga, Colombia; orcid.org/0000-0002-7897-2526; Email: dmolina@uis.edu.co
550

551 Authors

552 **Keyner S. Núñez-Méndez** – Grupo de Recobro Mejorado,
553 GRM, Universidad Industrial de Santander-UIS, A.A. 678
554 Bucaramanga, Colombia

555 **Luis M. Salas-Chia** – Grupo de Recobro Mejorado, GRM,
556 Universidad Industrial de Santander-UIS, A.A. 678
557 Bucaramanga, Colombia

558 **Samuel F. Muñoz** – Grupo de Recobro Mejorado, GRM,
559 Universidad Industrial de Santander-UIS, A.A. 678
560 Bucaramanga, Colombia

561 **Paola A. León** – Grupo de Recobro Mejorado, GRM,
562 Universidad Industrial de Santander-UIS, A.A. 678
563 Bucaramanga, Colombia

564 **Adan Y. León** – Grupo de Recobro Mejorado, GRM and
565 Grupo de investigación en Corrosión, GIC, Universidad
566 Industrial de Santander-UIS, A.A. 678 Bucaramanga,
567 Colombia

568 Complete contact information is available at:

569 <https://pubs.acs.org/10.1021/acs.energyfuels.0c04142>

570 Notes

571 The authors declare no competing financial interest.

572 ■ ACKNOWLEDGMENTS

573 The authors acknowledge the financial support provided by the
574 Universidad Industrial de Santander (UIS) and their
575 professionals' staff according to Project No. 2681 (Capital
576 Semilla).

577 ■ REFERENCES

- 578 (1) Lang, L.; Li, H.; Wang, X.; Liu, N. *J. Pet. Sci. Eng.* **2020**, *185*,
579 106659.
580 (2) Castañeda, L.; Muñoz, J.; Ancheyta, J. *Fuel* **2012**, *100*, 110–127.
581 (3) Larter, S.; Head, I. *Elements* **2014**, *10* (4), 277–283.
582 (4) Wiehe, I.; Liang, K. *Fluid Phase Equilib.* **1996**, *117* (1–2), 201–
583 210.
584 (5) Babadagli, T. Philosophy of EOR. *J. Pet. Sci. Eng.* **2020**, *188*,
585 106930.
586 (6) Butler, R.; McNab, G.; Lo, H. *Can. J. Chem. Eng.* **1981**, *59* (4),
587 455–460.

- (7) Alvarado, V.; Manrique, E. *Energies* **2010**, *3*, 1529–1575. 588
(8) Sarathi, P. *In-Situ Combustion Handbook - Principles and* 589
Practices; National Petroleum Technology Office, Tulsa, OK, USA, 590
1999. 591
(9) Wu, Z.; Wang, L.; Xie, C.; Yang, W. *Fuel* **2019**, *252*, 109–115. 592
(10) Al Dasani, A.; Bai, B. *J. Pet. Sci. Eng.* **2011**, *79*, 10–24. 593
(11) Zhao, Y. *J. Pet. Sci. Eng.* **2020**, *189*, 107016. 594
(12) Wang, Y.; Ren, S.; Zhang, L.; Peng, X.; Pei, S.; Cui, G.; Liu, Y. 595
Fuel **2018**, *211*, 471–483. 596
(13) Mahmoud, M.; Alade, O. S.; Hamdy, M.; Patil, S.; Mokheimer, 597
E. M.A. *Energy Convers. Manage.* **2019**, *202*, 112203. 598
(14) Wang, K.; Yan, W.; Deng, J.; Tian, H.; Li, W.; Wang, Y.; Wang, 599
L.; Ye, S. *J. Pet. Sci. Eng.* **2018**, *167*, 241–248. 600
(15) Barroux, C.; Lamourux-Var, V. Using geochemistry to address 601
H₂ production risk due to steam injection in oil sands. *SPE Annual* 602
Technical Conference and Exhibition; Society of Petroleum Engineers, 603
2013. 604
(16) Barrios, J. Estimation of the H₂S formation under injection 605
conditions for the Orinoco oil belt. *SPE International Improved Oil* 606
Recovery Conference; Society of Petroleum Engineers, 2010. 607
(17) Hyne, J. *Aquathermolysis: a Synopsis of Work on the Chemical* 608
Reaction between Water (Steam) and Heavy Oil Sands during Simulated 609
Steam Stimulation; AOSTRA Library and Information Service, 1986. 610
(18) Liu, X.; Li, Y.; Zhang, Z.; Li, X.; Zhao, M.; Su, C. Synthesis of 611
silica/metatitanic acid nanocomposite and evaluation of its catalytic 612
performance for aquathermolysis reaction of extra-heavy crude oil. *J.* 613
Energy Chem. **2015**, *24* (4), 472–476. 614
(19) Yi, S.; Babadagli, T.; Li, H. Use of nickel nanoparticles for 615
promoting aquathermolysis reaction during cyclic steam stimulation. 616
SPE Annual Technical Conference and Exhibition; Society of Petroleum 617
Engineers, 2018. 618
(20) Chen, Y.; Yang, C.; Wang, Y. *J. Anal. Appl. Pyrolysis* **2010**, *89* 619
(2), 159–165. 620
(21) Zhong, L.; Liu, Y.; Fan, H. Liaohe extra-heavy crude oil 621
underground aquathermolytic treatments using catalyst and hydrogen 622
donors under steam injection conditions. *SPE Annual Technical* 623
Conference and Exhibition; Society of Petroleum Engineers, 2003. 624
(22) Jiang, S.; Liu, X.; Liu, Y.; Zhong, L. In situ upgrading heavy oil 625
by aquathermolytic treatment under steam injection conditions. *SPE* 626
Annual Technical Conference and Exhibition; Society of Petroleum 627
Engineers, 2005. 628
(23) Nares, H.; Schacht-Hernández, P.; Ramírez-Garnica, M.; 629
Cabrera-Reyes, M. Upgrading heavy and extraheavy crude oil with 630
ionic liquid. *SPE Annual Technical Conference and Exhibition*; Society 631
of Petroleum Engineers, 2007. 632
(24) Wang, Y.; Chen, Y.; He, J.; Li, P.; Yang, C. *Energy Fuels* **2010**, 633
24, 1502–1510. 634
(25) Chao, K.; Chen, Y.; Li, J.; Zhang, X.; Dong, B. *Fuel Process.* 635
Technol. **2012**, *104*, 174–180. 636
(26) Zhang, Z.; Barrufet, M.; Lane, R.; Mamora, D. Experimental 637
study of in-situ upgrading for heavy oil using hydrogen donors and 638
catalyst under steam injection condition. *SPE Annual Technical* 639
Conference and Exhibition; Society of Petroleum Engineers, 2012. 640
(27) Maity, K.; Ancheyta, J.; Marroquín, G. *Energy Fuels* **2010**, *24* 641
(5), 2809–2816. 642
(28) Betiha, M.; ElMetwally, A.; Al-Sabagh, A.; Mahmoud, T. *Energy* 643
Fuels **2020**, *34* (9), 11353–11364. 644
(29) Belgrave, J.; Moore, M.; Ursenbach, M. *J. Can. Petrol. Technol.* 645
1997, *36*, 38–44. 646
(30) Chao, K.; Chen, Y.; Liu, H.; Zhang, X.; Li, J. *Energy Fuels* **2012**, 647
26 (2), 1152–1159. 648
(31) Wu, C.; Lei, G.; Yao, C.; Jia, X. In situ upgrading extra-heavy oil 649
by catalytic aquathermolysis treatment using a new catalyst based 650
anamphiphilic molybdenum chelate. *SPE Annual Technical Conference* 651
and Exhibition; Society of Petroleum Engineers, 2010. 652
(32) Foss, L.; Petrukchina, N.; Kayukova, G.; Amerkhanov, M.; 653
Romanov, G.; Ganeeva, Y. *J. Pet. Sci. Eng.* **2018**, *169*, 269–276. 654

- 655 (33) Hao, H.; Su, H.; Chen, G.; Zhao, J.; Hong, L. Viscosity
656 reduction of heavy oil by aquathermolysis with coordination complex
657 at low temperature. *Open Fuels Energy Sci. J.* **2015**, *8*, 93–98.
- 658 (34) Hassanzadeh, H.; Galarraga, C.; Abedi, J.; Scott, C.; Chen, Z.;
659 Pereira-Almao, P. Modelling of bitumen ultradispersed catalytic
660 upgrading experiments in a batch reactor. *Canadian International*
661 *Petroleum Conference*; Petroleum Society of Canada, 2009.
- 662 (35) Kayukova, G.; Foss, L.; Feoktistov, D.; Vakhin, A.; Petrukhnina,
663 N.; Romanov, A. *Pet. Chem.* **2017**, *57* (8), 657–665.
- 664 (36) Olvera, J. N. R.; Gutierrez, G. J.; Serrano, J.A. R.; Ovando, A.
665 M.; Febles, V. G.; Arceo, L. D. B. *Catal. Commun.* **2014**, *43*, 131–135.
- 666 (37) Shuwa, S.; Al-Hajri, R.; Mohsenzadeh, A.; Al-Waheibi, M.;
667 Jibril, B. Heavy crude oil recovery enhancement and in situ upgrading
668 during steam using Ni-Co-Mo dispersed catalyst. *SPE EOR Conference*
669 *at Oil and Gas West*; Society of Petroleum Engineers, 2016.
- 670 (38) Sitnov, S.; Mukhamatdinov, I.; Vakhin, A.; Ivanova, A.;
671 Voronina, E. *J. Pet. Sci. Eng.* **2018**, *169*, 44–50.
- 672 (39) Hashemi, R.; Pereira, P. Experimental study of simultaneous
673 Athabasca bitumen recovery and upgrading using ultra dispersed
674 catalysts injection. *SPE Canadian Unconventional Resources Conference*;
675 Society of Petroleum Engineers, 2011.
- 676 (40) Lin, D.; Feng, X.; Wu, Y.; Ding, B.; Lu, T.; Liu, Y.; Chen, X.;
677 Chen, D.; Yang, C. *Appl. Surf. Sci.* **2018**, *456*, 140–146.
- 678 (41) Patel, H.; Shah, S.; Ahmed, R.; Ucan, S. Effects of nanoparticles
679 and temperature on heavy oil viscosity. *J. Pet. Sci. Eng.* **2018**, *167*,
680 819–828.
- 681 (42) Rodrigues, R.; Rocha, J.; Oliveira, L.; Dias, J.; Muller, E.;
682 Castro, E.; Filgueiras, P. *Chemom. Intell. Lab. Syst.* **2017**, *166*, 7–13.
- 683 (43) Lin, D.; Zhu, H.; Wu, Y.; Lu, T.; Liu, Y.; Chen, X.; Peng, C.;
684 Yang, C.; Feng, X. *Fuel* **2019**, *245*, 420–428.
- 685 (44) Vakhin, A.; Sitnov, S.; Mukhamatdinov, I.; Aliev, F.;
686 Kudryashov, S.; Afanasiev, I.; Petrashov, O.; Varfolomeev, M.;
687 Nurgaliev, D. *Pet. Sci. Technol.* **2018**, *36* (22), 1857–1863.
- 688 (45) Du, H.; Li, M.; Liu, D.; Ren, Y.; Duan, Y. *Appl. Petrochem. Res.*
689 **2015**, *5* (2), 89–98.
- 690 (46) Qin, W.; Xiao, Z. *Adv. Mater. Res.* **2012**, *608-609*, 1428–1432.
- 691 (47) Chen, Y.; Wang, Y.; Wu, C.; Xia, F. *Energy Fuels* **2008**, *22* (3),
692 1502–1508.
- 693 (48) Chen, Y.; Wang, Y.; Lu, J.; Wu, C. *Fuel* **2009**, *88* (8), 1426–
694 1434.
- 695 (49) Li, G.; Chen, Y.; An, Y.; Chen, Y. *Fuel Process. Technol.* **2016**,
696 *153*, 94–100.
- 697 (50) Zhang, J.; Han, F.; Yang, Z.; Zhang, L.; Wang, X.; Zhang, X.;
698 Jiang, Y.; Chen, K.; Pan, H.; Lin, R. *Energy Fuels* **2020**, *34* (5), 5426–
699 5435.
- 700 (51) León, A.; Guzmán, A.; Laverde, D.; Chaudhari, R.;
701 Subramaniam, B.; Bravo-Suárez, J. *Energy Fuels* **2017**, *31*, 3868–3877.
- 702 (52) Leon, A.-Y.; Guzman M, A.; Picon, H.; Laverde C, D.; Molina
703 V, D. *Energy Fuels* **2020**, *34* (8), 9231–9242.
- 704 (53) Chen, G.; Yuan, W.; Bai, Y.; Zhao, W.; Gu, X.; Zhang, J.; Jeje,
705 A. *Pet. Chem.* **2017**, *57* (5), 389–394.
- 706 (54) Khalil, M.; Liu, N.; Lee, R. *Ind. Eng. Chem. Res.* **2017**, *56* (15),
707 4572–4579.
- 708 (55) Huang, S.; Cao, M.; Cheng, L. *Energy Fuels* **2018**, *32* (4),
709 4850–4858.
- 710 (56) Yi, Y.; Li, S.; Ding, F.; Yu, H. *Pet. Sci.* **2009**, *6* (2), 194–200.
- 711 (57) Li, C.; Huang, W.; Zhou, C.; Chen, Y. *Fuel* **2019**, *257*, 115779.
- 712 (58) Banda-Cruz, E.; Padrón-Ortega, S.; Gallardo-Rivas, N.;
713 Páramo-García, U.; Díaz-Zavala, N.; Melo-Banda, A. *J. Eng. Technol.*
714 **2017**, *6* (1), 49–58.
- 715 (59) Muraza, O.; Galadima, A. *Fuel* **2015**, *157*, 219–231.
- 716 (60) Lee, H.; Park, S. *Kongop Hwahak* **2016**, *27* (4), 343–352.
- 717 (61) Suwaid, M.; Varfolomeev, M.; Al-Muntaser, A.; Yuan, C.;
718 Starshinova, V.; Zinnatullin, A.; Vagizov, F.; Rakhmatullin, I.;
719 Emelianov, D.; Chemodanov, A. *Fuel* **2020**, *281*, 118753.
- 720 (62) Kudryashov, S.I.; Afanasiev, I.S.; Petrashov, O.V.; Vakhin, A.V.;
721 Sitnov, S.A.; Akhmediayrov, A.A.; Varfolomeev, M.A.; Nurgaliev, D.K.
722 *Neft. Khoz.* **2017**, *2017* (8), 30–34.
- (63) Xu, Y.; Ayala-Orozco, C.; Wong, M. Heavy oil viscosity 723
reduction using iron III para-toluenesulfonate hexahydrate. *SPE* 724
Annual Technical Conference and Exhibition; Society of Petroleum 725
Engineers, 2018. 726
- (64) Wu, C.; Lei, G.-L.; Yao, C.-j.; Sun, K.-j.; Gai, P.-y.; Cao, Y.-b. *J.* 727
Fuel Chem. Technol. **2010**, *38* (6), 684–690. 728
- (65) Gu, X.; Zhang, F.; Chen, G.; Zhang, J.; Meng, M.; Li, B.; 729
Zhang, Z. *Russ. J. Appl. Chem.* **2016**, *89* (12), 2061–2065. 730
- (66) Xu, H.; Pu, C. *J. Fuel Chem. Technol.* **2011**, *39* (8), 606–610. 731
- (67) Wang, Y.; Chen, Y.; He, J.; Li, P.; Yang, C. *Energy Fuels* **2010**, 732
24, 1502–1510. 733
- (68) Avbenake, O.; Al-Hajri, R.; Jibril, B. *Pet. Sci. Technol.* **2020**, *38* 734
(14), 800–807. 735
- (69) Meléndez, L.; Lache, A.; Orrego-Ruiz, J.; Pachón, Z.; Mejía- 736
Ospino, E. *J. Pet. Sci. Eng.* **2012**, *90*, 56–60. 737
- (70) Mohammadi, M.; Khorrami, M.; Vatani, A.; Ghasemzadeh, H.; 738
Vatanparast, H.; Bahramian, A.; Fallah, A. *Spectrochim. Acta, Part A* 739
2020, *232*, 118157. 740
- (71) Douda, J.; Alvarez, R.; Bolaños, N. *Energy Fuels* **2008**, *22*, 741
2619–2628. 742
- (72) Chen, M.; Li, C.; Li, G.; Chen, Y.; Zhou, C. *Pet. Sci.* **2019**, *16* 743
(2), 439–446. 744
- (73) Tverdov, I.; Khafizov, N.; Madzhidov, T.; Varfolomeev, M.; 745
Yuan, C.; Kadkin, O. *ACS Omega* **2020**, *5* (31), 19589–19597. 746